ELSEVIER

Journal of Organometallic Chemistry 491 (1995) 247–253

Journal of Organometallic Chemistry

The X-ray crystal structures of $ClPh_2SnFe(CO)_3(NO)$ and $Ph_3SnFe(CO)_3(NO)$ and a re-investigation of the IR spectra of $XR_2SnFe(CO)_3(NO)$ species

Mayson Kay, Kenneth M. Mackay, Brian K. Nicholson *

School of Science and Technology, University of Waikato, Hamilton, New Zealand

Received September 9, 1994

Abstract

A range of complexes $Cl_{3-n}R_nSnFe(CO)_3(NO)$ (R = Ph, Me; $n = 0$–3) has been prepared, and the X-ray crystal structures of $Ph_3SnFe(CO)_3(NO)$ (Sn–Fe 2.619 Å) and $ClPh_2SnFe(CO)_3(NO)$ (Sn–Fe 2.582 Å) have been determined. The complex IR spectra of the species with mixed substituents on tin are discussed in terms of conformers related by rotation about the Sn–Fe bond, which gives rise to different delocalised π-bonding interactions. Comparison with earlier work suggests the previously reported germanium complexes $R_2Ge(\mu\text{-}X)Fe(CO)_2(NO)$ do not exist.

Keywords: Tin; Iron; Carbonyl; Nitrosyl; Crystal structure; Infrared spectroscopy

1. Introduction

The first well-characterised complexes which incorporated a halogen-bridged M–M′ bond (M = transition metal, M′ = Group 14 element) were reported by Kummer and Graham [1]. They were of the form $L_5M(\mu\text{-}X)M'R_3$, with seven-coordinate M and five-coordinate M′, as in **1**. Further examples containing Mo and W have been investigated more recently by other groups [2]. An iridium-containing example, $BrMe_2Sn(\mu\text{-}Br)Ir[2\text{-}(Me_2NCH_2C_6H_4](COD)$, has also been fully characterised, and was discussed as a "trapped" three-centre intermediate in the oxidative addition of an R_3Sn–Br species [3]. A different class of halogen-bridged M–M′ bonds has been established crystallographically for *cis*-$[RhCl\{M'(NR_2)_2\}(PPh_3)_2]$ (M = Ge, Sn; R = $SiMe_3$), in which the Cl bridges the Rh–M′ bond to give a formally four-coordinate M′ atom [4]. This last class has an apparent precedent in complexes reported in 1972 by Curtis and Job [5], who treated R_2GeX_2 with $[Fe(CO)_3(NO)]^-$ to give products characterised as **2**. This formulation was supported by micro-analytical [6*] and mass spectrometric data, and the halogen-bridged Fe–Ge bond was invoked to explain the complexity of the ν_{CO} and ν_{NO} spectra. However there was no obvious reason why compounds of type **2** should be formed under such mild conditions (rather than the expected $XR_2GeFe(CO)_3(NO)$ with unbridged M–M′) whereas the iso-electronic species $XR_2GeCo(CO)_4$ did not show any tendency to eliminate CO and form a halogen-bridged bond. Furthermore, Casey and Manning [7] have reported tin analogues which were assigned as non-bridged $XR_2SnFe(CO)_3(NO)$ (**3**). We have therefore re-investigated these reactions and have characterised $Ph_3SnFe(CO)_3(NO)$ and $ClPh_2SnFe(CO)_3(NO)$ by X-ray crystallography. We conclude that compounds **2** probably do not exist, and offer an alternative interpretation of the IR spectra.

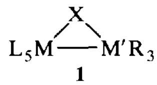

1

M = Mo, W; M′ = Ge, Sn

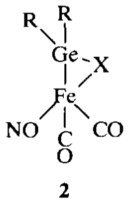

2

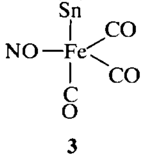

3

2. Experimental details

Reactions were performed under nitrogen in standard Schlenk equipment. Carbonyl region IR spectra were recorded as solutions in petroleum spirit (bp 60–80°C) on a Digilab FTS-45 FT-IR, and NMR spec-

---

* Corresponding author.

SSDI 0022-328X(94)05251-4

Table 1
IR spectral data as solutions in petroleum spirits, 2100–1700 cm^{-1}

$R_3EFe(CO)_3(NO)$ compounds	ν(CO)					ν(NO)	
$Ph_3SnFe(CO)_3(NO)$	2065(s)		2011(s)		1979(s)	1774(s)	
$Me_3SnFe(CO)_3(NO)$	2062(s)		2002(s)		1969(s)	1765(s)	
$Cl_3SnFe(CO)_3(NO)$ [a]	2101		2058		2032	1825	
$Br_3SnFe(CO)_3(NO)$ [a]	2098		2054		2028	1820	
$Cl_3GeFe(CO)_3(NO)$	2104(s)		2061(s)		2036(s)	1828(s)	
$Ph_3GeFe(CO)_3(NO)$ [b]	2073		2020		1990	1783	
$XR_2EFe(CO)_3(NO)$ compounds:	ν(CO)					ν(NO)	
$ClPh_2SnFe(CO)_3(NO)$	2076(s)	2029(m)	2026(s)	2002(s)	1989(s)	1976(s)	1777(s)
$Cl_2PhSnFe(CO)_3(NO)$	2089(s)	2044(m)	2036(m)	2012(s)	2006(sh)	1817(s)	1802(s)
$ClMe_2SnFe(CO)_3(NO)$	2075(s)	2026(m)	2021(m)	1996(s)	1984(s)	1789(s)	1772(s)
$Cl_2MeSnFe(CO)_3(NO)$	2089(s)	2045(s)	2037(m)	2008(sh)	2004(s)	1819(s)	1797(s)
$I_2MeSnFe(CO)_3(NO)$	2083(s)	2039(s)	2032(m)	2005(s)	1999(s)	1809(s)	1792(s)
$ClMe_2GeFe(CO)_3(NO)$ [c]	2082	2028		1997	1990	1797	1777
$ViCl_2GeFe(CO)_3(NO)$ [c,d]	2095	2051	2044	2022	2013	1819	1804

[a] Ref. [7]. [b] Ref [9]. [c] Ref [5]. [d] Vi = vinyl; a peak at 2074 cm^{-1} is also reported.

tra on a Bruker AC300 spectrometer in $CDCl_3$. Mass spectra were obtained from a VG 70-SE machine. The source of solutions of the $[Fe(CO)_3(NO)]^-$ ion was $Hg[Fe(CO)_3(NO)]_2$, prepared by a published method [8]. The preparation of the complexes of interest followed that previously reported for the phenyl/chloro/tin examples [7,9]. A typical preparation is given below in detail, and others were obtained in a directly analogous fashion. Solid phase IR, ^1H, ^{13}C and ^{119}Sn NMR, and mass spectrometry details are given below, where available, and ν(CO) and ν(NO) data for solutions are given in Table 1.

2.1. Preparation of $Ph_3SnFe(CO)_3(NO)$

A solution of $Hg[Fe(CO)_3NO]_2$ (0.33 g, 0.6 mmol) in diethyl ether (30 ml) was reduced by stirring for 1 h over an excess of sodium amalgam (1%). The red solution had become yellow, showing that the reduction to $Na[Fe(CO)_3NO]$ was complete. The solution was decanted from the amalgam under N_2 in to another Schlenk flask containing Ph_3SnCl (0.39 g, 1 mmol). The formation of a white precipitate was immediately evident. After 1 h of stirring, the solvent was removed under vacuum and the product extracted with petroleum spirit (30 ml), from which light-orange crystals of $Ph_3SnFe(CO)_3(NO)$ were obtained [7,9]. IR: (KBr disc) ν(CO) 2066 (s), 2009 (s), 1966 (s); ν(NO) 1766 (s) cm^{-1}. ^1H NMR: δ 7.43–7.66 (multiplet). ^{13}C NMR: δ 208.7 (s), 140.1 (s), 136.5 ($^2J_{C-Sn}$ = 42 Hz), 129.5 (s), 128.9 ($^3J_{C-Sn}$ = 63 Hz). ^{119}Sn NMR: δ 41.6 ($\nu_{1/2}$ 7 Hz). Mass spectrum: 521 (M^+), 493 (M^+-CO), 437 (M^+-3CO), 407 (Ph_3SnFe), 351 (Ph_3Sn^+), 197 ($PhSn^+$). The compound was fully characterised by an X-ray crystal structure determination.

2.2. Preparation of $Ph_2ClSnFe(CO)_3(NO)$

Recrystallised from petroleum spirit to give orange crystals [7]. Anal. Found: C, 37.77; H, 2.11; N, 2.80. $C_{12}H_{10}NO_4SnFe$ calc.: C, 37.67; H, 2.11; N, 2.93%. IR: (KBr disc) ν(CO) 2080 (s), 2029 (m), 2018 (m), 2004 (m), 1993 (m), 1969 (s,br); ν(NO) 1793 (s), 1753 (s) cm^{-1}. ^1H NMR: δ 7.48–7.71 (m). ^{13}C NMR: δ 206.4 (s), 142.3 (s), 135.0 ($^2J_{C-Sn}$ = 53 Hz), 130.6 ($^4J_{C-Sn}$ = 14 Hz), 129.3 ($^3J_{C-Sn}$ = 64 Hz). ^{119}Sn NMR: δ 159.7 ($\nu_{1/2}$ 30 Hz). Mass spectrum: 451 (M^+-CO), 444 (M^+-Cl), 423 (M^+-2CO), 416 (M^+-CO-Cl), 395 (M^+-3CO), 360 (M^+-3CO-Cl), 309 (Ph_2ClSn^+), 197 ($PhSn^+$), 155 ($ClSn^+$). A full X-ray crystal structure analysis was carried out.

2.3. Preparation of $PhCl_2SnFe(CO)_3(NO)$

Recrystallised from petroleum spirit to give orange crystals [7]. IR: (KBr disc) ν(CO) 2094 (s), 2043 (s), 2014 (sh), 2003 (s); ν(NO) 1812 (s), 1793 (s) cm^{-1}. ^1H NMR: δ 7.53–7.70 (m). ^{13}C NMR: δ 203.8 (s), 135.0 (s), 133.6 ($^2J_{C-Sn}$ = 33 Hz), 131.6 (s), 129.8 ($^3J_{C-Sn}$ = 32 Hz). ^{119}Sn NMR 170.8 ($\nu_{1/2}$ 75 Hz). Mass spectrum: 409 (M^+-CO), 402 (M^+-Cl), 381 (M^+-2CO), 374 (M^+-CO-Cl), 353 (M^+-3CO), 344 (M^+-2CO-Cl), 323 ($ClPh_2SnFe^+$), 288 (Ph_2SnFe^+), 267 ($PhCl_2Sn^+$), 232 ($PhClSn^+$), 197 ($PhSn^+$), 155 ($ClSn^+$).

2.4. Preparation of $Me_3SnFe(CO)_3(NO)$

Recrystallization from petroleum spirit afforded air-sensitive orange-red crystals. ^1H NMR: δ 0.66 (s). ^{13}C NMR: δ-0.95 (s). ^{119}Sn NMR: δ 171.7 (s).

2.5. Preparation of $Me_2ClSnFe(CO)_3(NO)$

Recrystallization from petroleum spirit afforded orange crystals. ^1H NMR: δ 1.16 ($^2J_{Sn-H}$ = 50 Hz). ^{13}C NMR: δ 206.8 ($^2J_{Sn-C}$ = 41 Hz), 5.50 ($^1J_{^{117}Sn-^{13}C}$ = 290 Hz, $^1J_{^{119}Sn-^{13}C}$ = 303 Hz). ^{119}Sn NMR: δ 305.7 ($\nu_{1/2}$ 39 Hz). Mass spectrum: 327 (M^+-CO), 299 (M^+-2CO), 271

(M^+-3CO), 241 (M^+-3CO-NO), 185 (Me_2ClSn^+), 170 ($Fe(CO)_3NO^+$), 155 ($ClSn^+$), 135 ($MeSn^+$).

2.6. Preparation of $MeCl_2SnFe(CO)_3(NO)$

Recrystallization from petroleum spirit afforded orange crystals, characterised by IR spectroscopy.

2.7. Preparation of $MeI_2SnFe(CO)_3(NO)$

Recrystallization from petroleum spirit afforded red crystals, characterised spectroscopically.

2.8. X-ray crystal structure of $Ph_3SnFe(CO)_3(NO)$.

Orange crystals of $Ph_3SnFe(CO)_3(NO)$ were obtained by recrystallization from petroleum spirit. Preliminary precession photography indicated triclinic symmetry, so the space group $P\bar{1}$ was assumed and was confirmed by the successful refinement. Cell constants and intensity data were obtained on a Enraf Nonius CAD4 four-circle diffractometer at 23°C.

2.8.1. Crystal data

$C_{21}H_{15}FeNO_4Sn$, $M = 519.90$, triclinic; space group $P\bar{1}$, $a = 10.089(1)$ Å, $b = 10.501(1)$ Å, $c = 10.989(1)$ Å, $\alpha = 94.89(1)°$, $\beta = 110.66(1)°$, $\gamma = 82.00(1)°$, $U = 1077.9$ Å^3, $D_c = 1.602$ g cm^{-3} for $Z = 2$, $F(000) = 512$, μ(Mo-K$_\alpha$) = 17.7 cm^{-1}. Total of 3380 unique data, $0° < 2\theta < 50°$, 3342 data with $I \geq 3\sigma(I)$, corrected for absorption using an empirical method, used for all calculations. The Fe and Sn atom positions were revealed by automatic analysis of the Patterson map using SHELXS-86 [10]. All other non-hydrogen atoms were located in a subsequent difference map. In the final cycle of full-matrix least-squares refinement all non-hydrogen atoms were assigned anisotropic temperature factors and H atoms were included in their calculated positions with common isotropic temperature factors for each type. The refinement converged with $R = 0.0308$, $R_w = 0.0361$ where $w = [\sigma(F)^2 + 0.00142F^2]^{-1}$ and with no parameter shifting more than 0.002σ. A final difference map showed no peaks or troughs greater than 0.62 e Å^{-3}. Atom parameters are given in Table 2, and selected bond lengths and angles are in Table 3. The structure is illustrated in Fig. 1.

For this structure and that considered below, tables of thermal parameter and hydrogen coordinates, and complete lists of bond lengths and angles have been deposited at the Cambridge Crystallographic Data Centre.

Table 2
Final positional and U_{eq} values for $Ph_3SnFe(CO)_3(NO)$

Atom	x	y	z	U_{eq} [a]
Sn(1)	0.12073(2)	0.30260(2)	0.31489(2)	0.058
Fe(1)	0.2337(1)	0.1338(1)	0.1789(1)	0.075
C(1) [b]	0.2008(5)	0.2636(4)	0.0768(4)	0.076
C(2) [b]	0.0885(5)	0.0541(4)	0.1674(4)	0.071
C(3) [b]	0.3841(4)	0.1302(4)	0.3237(4)	0.070
C(4)	0.3133(6)	0.0146(5)	0.0852(5)	0.087
C(11)	0.2435(5)	0.3239(5)	0.6129(4)	0.082
C(12)	0.2901(6)	0.2864(8)	0.7391(5)	0.114
C(13)	0.2887(8)	0.1624(9)	0.7645(7)	0.134
C(14)	0.2342(9)	0.0775(7)	0.6659(8)	0.135
C(15)	0.1850(7)	0.1145(5)	0.5366(5)	0.102
C(16)	0.1889(4)	0.2380(4)	0.5098(4)	0.068
C(21)	0.0913(5)	0.5942(5)	0.2977(6)	0.093
C(22)	0.1298(6)	0.7157(5)	0.3014(7)	0.120
C(23)	0.2676(8)	0.7315(5)	0.3250(6)	0.115
C(24)	0.3665(7)	0.6295(6)	0.3468(7)	0.118
C(25)	0.3279(5)	0.5036(5)	0.3433(7)	0.103
C(26)	0.1892(4)	0.4868(3)	0.3182(3)	0.062
C(31)	−0.1857(5)	0.3067(5)	0.3114(5)	0.087
C(32)	−0.3319(6)	0.3205(6)	0.2597(8)	0.114
C(33)	−0.4020(6)	0.3500(6)	0.1310(9)	0.123
C(34)	−0.3291(6)	0.3635(6)	0.0551(7)	0.110
C(35)	−0.1779(5)	0.3516(5)	0.1045(5)	0.090
C(36)	−0.1072(4)	0.3212(3)	0.2330(4)	0.066
O(1)	0.1810(5)	0.3478(4)	0.0117(4)	0.120
O(2)	−0.0078(4)	0.0032(4)	0.1570(4)	0.104
O(3)	0.4807(4)	0.1261(4)	0.4142(4)	0.109
O(4)	0.3647(6)	−0.0551(4)	0.0296(5)	0.130

[a] U_{eq} is defined as one third of the trace of the orthogonalized U_{ij} tensor.

[b] Each of these is 0.66C/0.33N from CO/NO disorder.

2.9. X-ray crystal structure of $Ph_2ClSnFe(CO)_3(NO)$

Orange crystals of $Ph_2ClSnFe(CO)_3NO$ were obtained by recrystallization from heptane. Preliminary precession photography indicated a C-centred monoclinic lattice with systematic absences consistent with either the space group $C2/c$ or Cc, the former proving to be correct by the successful refinement. Cell constants and intensity data were obtained on a Nicolet XRD P3 four-circle diffractometer at −153°C.

2.9.1. Crystal data

$C_{15}H_{10}ClFeNO_4Sn$, $M = 478.24$, monoclinic; space group $C2/c$ $a = 21.285(4)$ Å, $b = 11.666(3)$ Å, $c = 28.354(6)$ Å, $\beta = 96.17(1)°$, $U = 6999.8$ Å^3, $D_c = 1.77$ g cm^{-3} for $Z = 16$, $F(000) = 3712$, μ(Mo-Kα) = 23.2 cm^{-1}. A total of 6024 unique data for which $0° < 2\theta < 50°$ were used for all calculations after correction for absorption. The Fe, Sn and Cl atom positions of the two independent molecules in the asymmetric unit were revealed by automatic analysis of the Patterson map using SHELXS-86 [10]. All other non-hydrogen atoms were revealed by a subsequent difference map. A penultimate electron density map showed an isolated residual peak of approximately 2.5 e Å^{-3} at $x = 0.0$, $y = 0.093$, $z = 0.75$, but this could not be assigned to any sensible atom so was not included in the model. (Assignment as the O atom of a water of crystallisation molecule was deemed unlikely in a crys-

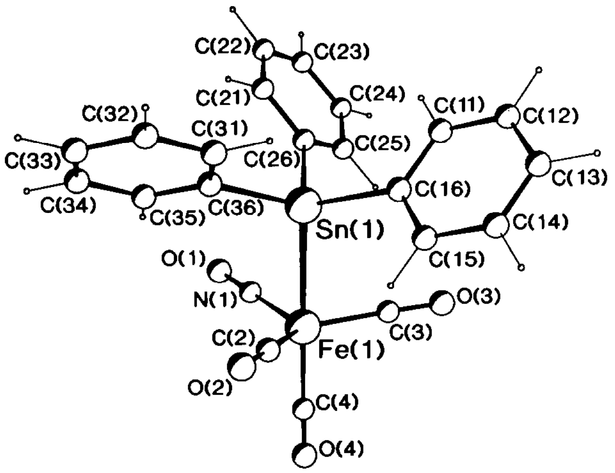

Fig. 1. The structure of $Ph_3SnFe(CO)_3(NO)$. The NO group is arbitrarily assigned to one of the equatorial sites.

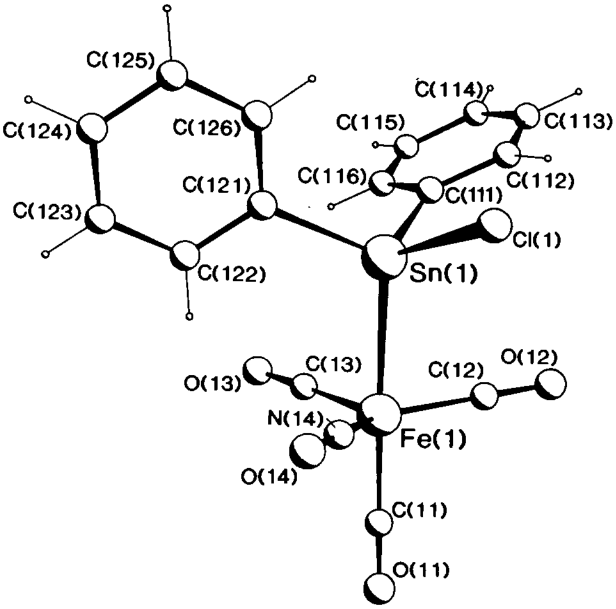

Fig. 2. The structure of one of the independent molecules of $ClPh_2SnFe(CO)_3(NO)$. The NO group is arbitrarily assigned to one of the equatorial sites.

tal with molecules containing hydrolysable Sn–Cl bonds). In the final cycle of full-matrix least-squares refinement all non-hydrogen atoms were assigned anisotropic temperature factors and H atoms were included in their calculated positions with common isotropic temperature factors for each type. The refinement converged with $R = 0.0305$, $R_w = 0.0280$ where $w = [\sigma(F)^2 + 0.00204F^2]^{-1}$ for all data, ($R = 0.0248$ for $I > 3\sigma(I)$ data). Atom parameters are given in Table 4, and selected bond lengths and angles are in Table 3. One of the two independent molecules is illustrated in Fig. 2.

Table 3

Selected bond parameters for $Ph_3SnFe(CO)_3(NO)$ and $ClPh_2SnFe(CO)_3(NO)$

$Ph_3SnFe(CO)_3(NO)$			
Bond lengths (Å)			
Sn(1)–Fe(1)	2.619(1)	Sn(1)–C(16)	2.144(4)
Sn(1)–C(26)	2.136(4)	Sn(1)–C(36)	2.140(4)
Fe(1)–C_{axial}	1.832(5)	Fe(1)–C_{equ} [a]	1.759(4)(av.)
Bond angles (°)			
Fe(1)–Sn(1)–C	109.8(1) (av.)	C–Sn(1)–C	109.2(1) (av.)
Sn(1)–Fe(1)–C_{equ} [a]	82.8(1) (av.)	Sn(1)–Fe(1)–C_{axial}	179.4(2)
$ClPh_2SnFe(CO)_3(NO)$			
Bond lengths (Å)			
	Molecule 1	Molecule 2	
Sn–Fe	2.577(1)	2.587(1)	
Sn–Cl	2.377(1)	2.387(1)	
Sn–C(11)	2.142(3)	2.135(3)	
Sn–C(21)	2.140(3)	2.146(3)	
Fe–C_{equ} [a]	1.774(4) (av.)	1.774(4) (av.)	
Fe–C_{axial}	1.838(4)	1.836(4)	
Bond angles (°)			
Fe–Sn–Cl	108.82(3)	106.18(3)	
Fe–Sn–C(11)	114.4(1)	115.4(1)	
Fe–Sn–C(21)	113.6(1)	113.6(1)	
C(11)–Sn–C(12)	111.8(1)	114.4(1)	
Sn–Fe–C(1) [a]	178.2(1)	175.7(1)	
Sn–Fe–C(2) [a]	81.8(1)	84.3(1)	
Sn–Fe–C(3) [a]	85.6(1)	85.8(1)	
Sn–Fe–C(4) [a]	85.7(1)	80.8(1)	

[a] Or N from NO/CO disorder

3. Results and discussion

The reactions of organotin halides with solutions containing the $[Fe(CO)_3(NO)]^-$ ion proceeded smoothly according to eqn. 1 to give products of type **3**, as expected from earlier work involving the phenylchloro complexes [7,9].

$$R_nSnCl_{4-n} + [Fe(CO)_3(NO)]^- \rightarrow Cl_{3-n}R_nSnFe(CO)_3(NO)\ (\mathbf{5}) + Cl^- \qquad (1)$$

The methyl derivatives $Cl_nMe_{3-n}SnFe(CO)_3(NO)$, reported for the first time here, are much more air-sensitive than the phenyl analogues, but otherwise have similar properties.

IR spectral data in the 2100–1700 cm^{-1} region for the complexes prepared in this study are listed in Table 1, together with those for selected examples from earlier work [5,7,9]. The complexes fall into two categories. Those with a symmetrical substituent R_3Sn- show three carbonyl stretches and one nitrosyl band, and can therefore be assigned, as previously discussed, to a trigonal bipyramidal molecule with the R_3Sn substituent in an axial position and the nitrosyl equatorial [7,9]. The molecules with unsymmetrical substituents of the type XR_2Sn- show more complex spectra, however, with at least five ν(CO) and two ν(NO) bands. This spectral pattern is closely similar to those reported for germanium analogues by Curtis and Job [5], who attributed the complexity to isomers arising from a halogen-bridged Ge–Fe bond in a molecule of formula $R_2Ge(\mu\text{-}X)Fe(CO)_2(NO)$, as in **2**. In contrast Casey and Manning [7] attributed the spectra to conformers arising from restricted rotation about the Sn–Fe bond in molecules of structure **3**. To provide a definite answer we have carried out the structural determination for both a symmetrical and an unsymmetrical example, namely $Ph_3SnFe(CO)_3(NO)$ and $ClPh_2SnFe(CO)_3(NO)$.

The structure of $Ph_3SnFe(CO)_3(NO)$ is illustrated in Fig. 1. It shows the expected trigonal-bipyramidal structure, with the tetrahedrally coordinated tin substituent in the axial site. It is therefore of the same structural type as the iso-electronic $Ph_3SnCo(CO)_4$ [11]. It was not possible to distinguish crystallographically between the NO and the CO ligands, but it is known that NO ligands preferentially occupy equatorial sites in trigonal bipyramidal metal carbonyls [12], and the IR spectra also support this assignment, so the NO group has been arbitrarily assigned to equatorial site 1 for the purposes of discussion. In fact the NO ligand is almost certainly disordered across all three equatorial sites. The conformation of the Ph_3Sn group is staggered with respect to the equatorial groups on the iron atom, as expected on steric grounds.

The Sn–Fe bond length of 2.619(1) Å is at the longer end of the range known for such bonds; only those in the crowded octahedral complex $(Ph_3Sn)_2Fe(CO)_4$ [2.660(1) Å] exceed it [13]. The Sn–C bonds are within the normal range [14], and the $Fe\text{–}C/N_{eq}$ bond lengths (av. 1.759 Å) are shorter than the $Fe\text{–}C_{ax}$ one (1.832 Å). This is normal for trigonal bipyramidal molecules, and the effect is perhaps enhanced in this molecule because of the contribution to the equatorial Fe–C lengths of the disordered shorter Fe–N component.

Table 4
Final positional and U_{eq} values for $ClPh_2SnFe(CO)_3(NO)$.

Atom	x	y	z	U_{eq} [a]
Sn(1)	0.1243(1)	0.0575(1)	0.6786(1)	0.024(1)
Fe(1)	0.0062(1)	0.0841(1)	0.6500(1)	0.039(1)
Cl(1)	0.1369(1)	0.0479(1)	0.7628(1)	0.039(1)
C(11)	−0.0787(2)	0.1018(3)	0.6314(1)	0.031(1)
O(11)	−0.1312(1)	0.1114(2)	0.6197(1)	0.038(1)
C(12) [b]	0.0008(2)	−0.0495(3)	0.6784(1)	0.033(1)
O(12)	−0.0028(1)	−0.1370(3)	0.6961(1)	0.058(1)
C(13) [b]	0.0305(2)	0.0920(3)	0.5924(1)	0.027(1)
O(13)	0.0457(1)	0.0999(3)	0.5550(1)	0.049(1)
C(14) [b]	0.0128(2)	0.2170(4)	0.6816(1)	0.035(1)
O(14)	0.0156(2)	0.3034(3)	0.6997(1)	0.068(1)
C(111)	0.1633(2)	−0.1021(3)	0.6583(1)	0.026(1)
C(112)	0.1785(2)	−0.1909(3)	0.6907(1)	0.038(1)
C(113)	0.2049(2)	−0.2920(3)	0.6757(2)	0.043(1)
C(114)	0.2161(2)	−0.3062(3)	0.6290(2)	0.039(1)
C(115)	0.2007(2)	−0.2189(3)	0.5965(2)	0.042(1)
C(116)	0.1748(2)	−0.1173(3)	0.6114(1)	0.033(1)
C(121)	0.1818(2)	0.1998(3)	0.6626(1)	0.025(1)
C(122)	0.1579(2)	0.2886(3)	0.6327(1)	0.030(1)
C(123)	0.1967(2)	0.3785(3)	0.6217(1)	0.034(1)
C(124)	0.2595(2)	0.3812(3)	0.6414(1)	0.034(1)
C(125)	0.2835(2)	0.2933(3)	0.6715(1)	0.031(1)
C(126)	0.2451(2)	0.2031(3)	0.6818(1)	0.027(1)
Sn(2)	0.3900(1)	0.0251(1)	0.5866(1)	0.024(1)
Fe(2)	0.4698(1)	0.1759(1)	0.5624(1)	0.035(1)
Cl(2)	0.4292(1)	−0.1568(1)	0.5647(1)	0.037(1)
C(21)	0.5265(2)	0.2771(3)	0.5411(1)	0.033(1)
O(21)	0.5607(1)	0.3411(3)	0.5273(1)	0.047(1)
C(22) [b]	0.5261(2)	0.0958(3)	0.6005(1)	0.029(1)
O(22)	0.5618(1)	0.0463(3)	0.6258(1)	0.048(1)
C(23) [b]	0.4238(2)	0.2761(3)	0.5891(1)	0.023(1)
O(23)	0.3946(1)	0.3435(2)	0.6066(1)	0.042(1)
C(24) [b]	0.4423(2)	0.1217(3)	0.5051(1)	0.026(1)
O(24)	0.4231(1)	0.0902(3)	0.4682(1)	0.042(1)
C(211)	0.3843(2)	0.0092(3)	0.6610(1)	0.026(1)
C(212)	0.4157(2)	0.0851(3)	0.6937(1)	0.031(1)
C(213)	0.4097(2)	0.0734(4)	0.7421(1)	0.039(1)
C(214)	0.3738(2)	−0.0150(4)	0.7578(1)	0.039(1)
C(215)	0.3428(2)	−0.0912(3)	0.7257(1)	0.038(1)
C(216)	0.3480(2)	−0.0795(3)	0.6773(1)	0.033(1)
C(221)	0.3002(2)	0.0313(3)	0.5443(1)	0.027(1)
C(222)	0.2812(2)	−0.0556(3)	0.5121(1)	0.036(1)
C(223)	0.2216(2)	−0.0526(4)	0.4865(1)	0.044(1)
C(224)	0.1809(2)	0.0370(4)	0.4923(1)	0.041(1)
C(225)	0.1996(2)	0.1253(4)	0.5234(1)	0.039(1)
C(226)	0.2589(2)	0.1227(3)	0.5495(1)	0.032(1)

[a] U_{eq} is defined as one third of the trace of the orthogonalized U_{ij} tensor.

[b] Each of these is 0.66C/0.33N from CO/NO disorder.

The angles between the substituents on the tin atom deviate by less than 2° from regularly tetrahedral, consistent with bonding to four bulky groups of similar electronegativity. The three equatorial ligands on the iron atom bend towards the tin substituent with an average Sn–Fe–C/N_{eq} angle of 82.8°. This effect is common in molecules of this type, and has been attributed to both steric and electronic effects [14,15].

The structure of $ClPh_2SnFe(CO)_3(NO)$ revealed two independent molecules in the asymmetric unit, but there were only minor differences between them, and so the discussion is based on average values of parameters. Fig. 2 shows that the structure is exactly analogous to that of $Ph_3SnFe(CO)_3(NO)$, with one Ph group replaced by a Cl. There is no bridging of the Sn–Fe bond by the Cl ligand. Again the NO ligand could not be distinguished, and so is arbitrarily assigned to one of the equatorial sites, although disorder is almost certainly present. The main effect of the presence of a Cl group is to shorten the Fe–Sn bond by 0.04 Å compared with that in the Ph_3Sn complex, and to distort the coordination around Sn from tetrahedral, giving Cl–Sn–C angles of 103°. Otherwise structural features are as discussed above for the more symmetrical example. For the purposes of the later discussion it is noteworthy that the three substituents on Sn are again staggered with respect to the equatorial groups on Fe, so that there is a Cl–Sn–Fe–C/Neq torsion angle of ca. 180° in both independent molecules. There are no obvious non-bonded interactions between the substituents on Sn and the equatorial ligands on Fe that would give rise to restricted rotation about the Sn–Fe bond, although clearly the staggered conformation is preferred.

The close matching of the IR spectra makes it clear that the tin compounds investigated here are directly comparable to the germanium compounds previously reported, but the structural results mean that the explanation of the complexity of the IR spectra of the unsymmetrical examples in terms of halogen-bridged isomers [5] is no longer tenable. An alternative explanation in terms of axial/equatorial positioning of the NO group can also be discounted, because there is no evidence for such isomers in the end-members of the series, with Ph_3Sn or Cl_3Sn substituents, and equatorial preference for NO is well established [12]. The only remaining explanation, as first proposed by Casey and Manning [7] is in terms of conformers with long lifetimes on the IR time-scale, related by a rotation about the Sn–Fe bond, with the unique group on the Sn atom either *anti* or *gauche* to the NO ligand on Fe. These two conformers then give rise to a clear separation of the ν(NO) band and the two lower energy ν(CO) bands, although no splitting of the highest energy ν(CO) band is resolved in any of the examples. Hence there are essentially two species in solution, one with (for the Ph_2ClSn- example) ν 2076, 2029, 2002, and 1796 cm^{-1}, and the other with ν 2076, 2026, 1989, and 1777 cm^{-1}.

The mechanism by which the two conformers give rise to such large separations is of interest, as are the different magnitudes of the splitting. For example, in $ClPh_2SnFe(CO)_3(NO)$ the ν(NO) is split by 19 cm^{-1}, the lowest ν(CO) by 13 cm^{-1} and the middle ν(CO) by 3 cm^{-1}, while the remaining band appears unresolved into two components. A simple through-space interaction of the substituents about the tin atom with the equatorial groups would be unlikely to cause a sufficient change in the molecular force fields to affect the stretching frequency to the extent observed. Similarly, a mechanism based on the unequal steric properties of the substituents on Sn seems unlikely, because the splittings for the Me/Cl series are similar to those of the Ph/Cl series where the difference in size is greater. An explanation based on electronic changes transferred through σ bonds is also not possible because these would not depend on specific conformations.

A more interesting proposal focuses attention on the question of π-bonding in the Sn–Fe bond. There has been much discussion concerning the possibility of back-donation of π electron density from the filled 3d orbitals on a transition metal M to the empty 3d or σ^* orbitals on a M′ atom (M′ = Si, Ge, Sn) in M–M′ bonds, although unambiguous evidence for or against such interation has been elusive [14–16]. For $XR_2SnFe(CO)_3(NO)$ molecules the 3d orbitals of Fe will be involved in π bonding to the CO/NO ligands, so any change in the Sn–Fe π-bonding would be expected to affect the Fe–C and Fe–N bonding (and hence the corresponding CO or NO stretching frequencies, because these are sensitive to π bonding changes). The possible effects of different conformers on Fe–Sn π bonding is illustrated in Fig. 3. For clarity only one dπ orbital is shown although the others will show corresponding effects. In conformer I the σ^* orbital overlapping with the dπ orbital is that associated with the Sn–Cl bond, whereas in II it is that of a Sn–C bond.

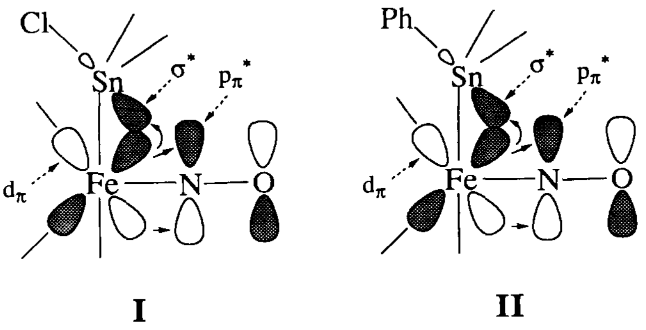

Fig. 3. A representation of the possible extended π-bonding $\sigma^* \rightarrow d\pi \rightarrow p\pi^*$ interactions for the two conformations in $ClPh_2SnFe(CO)_3(NO)$.

The different energies of the two σ^* orbitals will lead to varying π bonding in the two conformers, and hence differing availability of the dπ electrons for back bonding to the CO/NO ligands. This model can also be used to rationalise qualitatively the magnitudes of the splittings of the IR bands. The axially coordinated CO group will be unaffected by the rotational position of the Sn group, which will minimise the splitting of the bands it contributes to, while the effect should be greatest for the NO group because it is a stronger π-acceptor than CO. Note that this model also distinguishes between dπ-σ^* and dπ-dπ back-bonding because the latter involves non-bonding d orbitals on tin which would not be affected in the same way.

The IR spectra in KBr discs of the unsymmetrical examples are again more complex than expected for molecules with one conformation, although interpretation is made more difficult by solid-state effects. Nevertheless it appears that the discussion of the solution spectra can be extended to the solid-state spectra. The presence of both conformers of $ClPh_2SnFe(CO)_3(NO)$ in the solid is also indicated by the inability to define a unique position for the equatorial NO ligand in the X-ray crystal structure determination.

The ^1H and ^{13}C NMR data for the complexes studied were unremarkable, other than that they showed no sign of any splitting arising from the conformer effects noted for the IR spectra. Thus $Me_2ClSnFe(CO)_3(NO)$ showed sharp single resonances for the CH_3 group even at low temperature. The ^{119}Sn spectra for the series $Cl_{3-n}Ph_nFe(CO)_3(NO)$ ($n = 1$-3) similarly gave single peaks, although the unsymmetrical examples gave wider signals. That of $PhCl_2SnFe(CO)_3(NO)$ with $\nu_{1/2} = 75$ Hz was notable, but even at -60°C no further splitting was found. The timescale of rotation about the Sn–Fe bond in these complexes therefore appears to lie between the limits for IR and NMR experiments.

The mass spectra of $Cl_{3-n}Ph_nSnFe(CO)_3(NO)$ ($n = 1$-3) and $ClMe_2SnFe(CO)_3(NO)$ were recorded. Only for the Ph_3Sn example was a parent peak observed, in all other cases the highest mass peak corresponded to loss of one CO(NO) group. For $ClPh_2SnFe(CO)_3(NO)$ and $Cl_2PhSnFe(CO)_3(NO)$ a clear series of ions showed that Cl loss competed with loss of CO/NO ligands, but this was not so for $ClMe_2SnFe(CO)_3(NO)$. All showed evidence for Sn–Fe bond cleavage with the appearance of peaks of the type R_3Sn^+.

Acknowledgements

We thank Prof. Ward Robinson (University of Canterbury) and Dr Cliff Rickard (University of Auckland) for collection of X-ray intensity data, and Dr Ralph Thomson for assistance with NMR. Funding from the New Zealand Foundation for Research, Science and Technology is gratefully acknowledged.

References and notes

[1] R. Kummer and W.A.G. Graham, *Inorg. Chem., 8* (1968) 1208; M. Elder and D. Hall, *Inorg. Chem., 8* (1969) 1268; M. Elder and D. Hall, *Inorg. Chem., 8* (1969) 1273.

[2] M. Cano, M. Panizo, J.A. Campo, J. Tornero and N. Menendez, *Polyhedron, 13* (1994) 1835; P.K. Baker and D. Kendrick, *J. Organometal. Chem., 466* (1994) 139 and references therein.

[3] A.A.H. van der Zeijden, G. van Koten, J.M.A. Wouters, W.F.A. Wijsmuller, D.M. Grove, W.J.J. Smeets and A.L. Spek, *J. Am. Chem. Soc., 110* (1988) 5354.

[4] M.F. Lappert and R.S. Rowe, *Coord. Chem. Rev., 100* (1990) 267.

[5] M.D. Curtis and R.C. Job, *J. Am. Chem. Soc., 94* (1972) 2153.

[6] The micro-analytical data reported in ref. 5 for $Cl_2(C_2H_3)$-$GeFe(CO)_3(NO)$ (Found: C, 17.8; H, 0.94; Ge, 21.6; Fe, 16.8%) actually fits the *tri*-carbonyl $C_5H_3GeFeO_4NCl_2$ (calc.: C, 17.64; H, 0.89; Ge, 21.3; Fe, 16.4%) more closely than the *di*-carbonyl $C_4H_3GeFeO_3NCl_2$ to which it was attributed (calc.: C, 15.4; H, 0.97; Ge, 23.2; Fe, 17.9%).

[7] M. Casey and A.R. Manning, *J. Chem. Soc., A* (1971) 256.

[8] R.B. King, *Organometallic Syntheses, 1* (1965) 165.

[9] A.J. Cleland, S.A. Fieldhouse, B.H. Freeland, C.D.M. Mann and R.J. O'Brien, *J. Chem. Soc., A* (1971) 736.

[10] G.M. Sheldrick, *SHELXS86*-Program for Solving Crystal Structures, University of Gottingen, 1986; *SHELX76*-Program for Crystal Structure Determination, University of Cambridge, 1976.

[11] D.J. Patmore and W.A.G. Graham, *Inorg. Chem., 7* (1968) 771.

[12] J.H. Enmark and R.D. Feltham, *Coord. Chem. Rev., 13* (1974) 339.

[13] R.K. Pomeroy, L. Vancea, H.P. Calhoun and W.A.G. Graham, *Inorg. Chem., 16* (1977) 1508.

[14] J.A. Zubieta and J.J. Zuckerman, *Progress Inorg. Chem., 24* (1978) 251; M.S. Holt, W.L. Wilson and J.H. Nelson, *Chem. Rev., 89* (1989) 11.

[15] M. Elian and R. Hoffmann, *Inorg. Chem., 14* (1975) 1058; A.D. Berry, E.R. Corey, A.P. Hagen, A.G. MacDiarmid, F.E. Saalfeld and B.F. Wayland, *J. Am. Chem. Soc., 92* (1970) 1940.

[16] K.M. Mackay and B.K. Nicholson, in G. Wilkinson, F.G.A. Stone and E. Abel (eds.), *Comprehensive Organometallic Chemistry*, Pergamon, Oxford, 1982, Ch. 4; D.S. Tilley, in S. Patai and Z. Rappoport (eds.), *The Chemistry of Organic Silicon Compounds*, Wiley, New York, 1989; see also A.G. Orpen and N.G. Connelly, *Organometallics, 9* (1990) 1206; R.J. Morris and G.S. Girolami, *Inorg. Chem., 29* (1990) 4167; G. Pacchioni and P.S. Bagus, *Inorg. Chem., 31* (1992) 4391 for related discussions on M–P d-σ^* bonding.